

# Robust Extended Complex Kalman Filter Based LQR Control Strategy of Shunt Active Power Filter

Rakhee Panigrahi<sup>1</sup> and Rajesh Kumar Patjoshi<sup>2</sup>

<sup>1</sup>Electrical Engg. Dept., Biju Patnaik University of Technology, Parala Maharaja Engineering

<sup>2</sup>Electronics and Communication Engg. Dept., National Institute of Science and Technology, Berhampur, India

College, Berhampur, India, rpanigrahi99@gmail.com, rajeshpatjoshi1@gmail.com

*Abstract:* This study offers a new approach for reference current estimation employing proposed robust extended complex Kalman filter (RECKF) alongside linear quadratic regulator (LQR) strategy in the development of a three-phase shunt active power filter (SAPF) system to enrich power quality. A mathematical model of SAPF is established where LQR methodology is applied for accuracy advancement and it is achievable owing to the incorporation of grid perturbations such as voltage distortion and measurement noise in the representation of the plant to be regulated. A new exponential function introduced in the RECKF algorithm facilitates estimation of the state space variables at the point of common coupling (PCC) and also for the estimation of current references needed for the realization of LQR considering above said grid perturbations. The major benefit behind this proposed RECKF-LQR based SAPF system is self-supervising dc-link voltage without concerning over external proportional integral (PI) controller. The proposed RECKF-LQR method is implemented utilizing MATLAB/SIMULINK and also real-time digital simulator Opal-RT is carried out to support the simulation results. The results attained employing the proposed SAPF system together with some variants of Kalman filters (Kalman filter (KF), extended KF (EKF) and extended complex KF (ECKF)) are evaluated and it is observed that the proposed RECKF-LQR methodology exhibits better performance in terms of percentage total harmonic distortion and reference tracking action in the SAPF system.

*Keywords:* Robust extended complex Kalman filter; shunt active power filter; linear quadratic regulator; power quality; grid perturbations.

## 1. Introduction

Active power filters find enormous industrial applications in view meeting the international power quality standards. Through compensation for load harmonics, voltage unbalances and reactive power, these filters assure nature of the source current to be near-sinusoidal and phase relationship of the source current along with the source voltage to be similar. Presently, enormous category of such filters are obtainable; however, the three-phase three wire shunt active power filter (SAPF) is the most commonly employed topology [1, 3].

The most widespread methodology to develop the controllers for a SAPF is to reproduce it as a plant which is to be monitored. The grid agitations such as measurement noise, current or voltage transients, frequency deviation and the inherent voltage perturbation at PCC are reflected in the mathematical model of the plant so that the controller must have proficiency to eradicate such perturbations. Moreover, the overall SAPF may possibly oscillate and even turn out to be unstable based upon the nature of turbulences. A resolution for this problem was explained in [2], where an optimum filtering scheme was applied for extracting information regarding harmonics cancellation, harmonics and displacement power factor correction, harmonics and unbalance compensation and harmonics with unbalance and displacement power factor correction. The LQR has extensively been operated through several appliances [4, 5, 7], where optimal regulation is necessitated. LQR implementation deals with state feedback, in which the state weighting matrices can be preferred such that the control output is planned to fulfil a performance criterion. In case of current controller techniques such as sliding mode, dead beat,

hysteresis [2, 3, 6] the inner current control loop of SAPF is associated with a cascade strategy which concerns an exterior loop having simple PI regulator for the dc bus voltage regulation. Conversely, LQR does not requisite any external PI controller loop; rather it is designed to minimise a performance index, which can diminish the control efforts or preserves the energy of state variables under control.

To obtain efficient SAPF performance, it is important to select a fast and foremost reference current estimation strategy in addition with current controller. Both linear and nonlinear Kalman filtering approaches [8-14] have drawn widespread attention, as they precisely estimate the amplitude, phase and frequency of a signal suppressed with noise and harmonics. Further, most of the existing estimation methods [15-19] have not taken into account for grid agitations such as harmonics, measurement noise, voltage distortion and frequency deviation. Henceforth, aiming at above-mentioned issues (harmonics, noise, voltage distortion), more attentions are drawn towards the growth of a new estimation algorithm, the robust extended complex Kalman

filter (RECKF), where a new weighted function  $e^{-(y-h(x))^2}$  has been introduced concerning all the above grid agitations. When any anomalous situation occurs, the amount of residual vector  $(y - h(x))$  will be increased twice owing to insertion of a “square term” in the suggested function; as a consequence, the impacts of anomaly may be decreased at a quicker level (almost twice) contrasted to the weighted function declared in [20, 21]. Therefore, with rapid convergence, the proposed RECKF algorithm affords improved estimations independent of all grid agitations in the SAPF.

With abovementioned point of views, our proposed RECKF-LQR method is aimed to be a proficient control approach in SAPF system. The main contributions of this paper are: (i) Lessening the impacts of distorted voltage at the PCC on the functioning of the SAPF system through designing LQR approach; (ii) Emerging efficient algorithm built upon RECKF for reference current estimation that can handle numerous grid perturbations such as measurement noise, frequency variation and voltage distortion.

Organisation of the paper is as follows: Section 2 presents problem formulation of the paper. Section 3 represents the mathematical modelling of SAPF with its controller design. The PCC state space variables estimation and the reference generation methods are presented in Section 4 and Section 5 respectively. In order to assess the performance of the proposed control scheme, extensive simulation results are presented in Section 6 and verified by Real-Time Opal-RT Lab. Finally, the conclusion is summarized in Section 7.

## 2. Description About Proposed RECKF-LQR Based SAPF

The schematic layout of proposed RECKF-LQR based SAPF model is presented through Figure. 1(a) and (b), where  $i_{Sabc}, i_{Labc}, i_{Fabc}, v_{abc}$  represent the source current, load current, filter current and PCC voltage for three phases respectively. The SAPF is designed to inject a current into the PCC such as to compensate the harmonic content of load and the compensation is considered under grid perturbations such as measurement noise and inherent voltage distortion at PCC. Therefore, the whole SAPF system is well-organized by the proposed RECKF-LQR based control strategy.

As per comparative study, four filtering algorithms such as KF, EKF, ECKF and proposed RECKF are employed to estimate in phase and in quadrature fundamental component of PCC voltages  $v_{abc}$ , fundamental amplitude of load currents  $i_{Labc}$  and source currents  $i_{Sabc}$ . These estimations facilitate in achieving the PCC voltages and their derivatives and also the reference currents [22]. Afterwards, LQR is designed along with the knowledge of the above state space variables as depicted in Figure 2a and b.

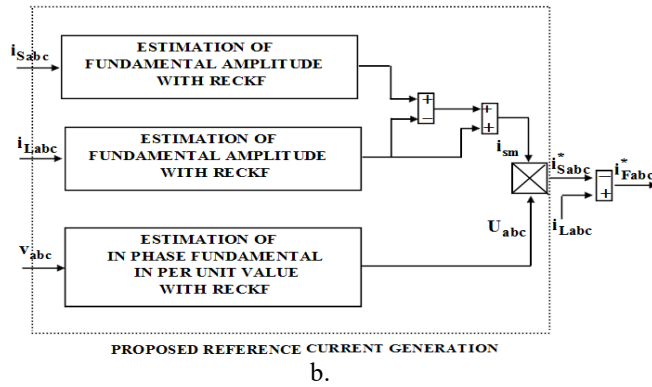
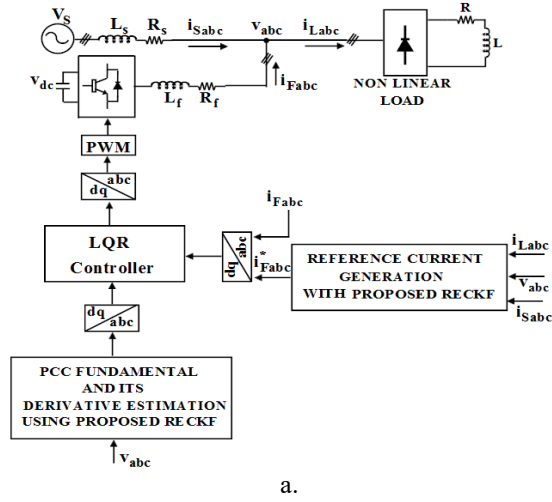
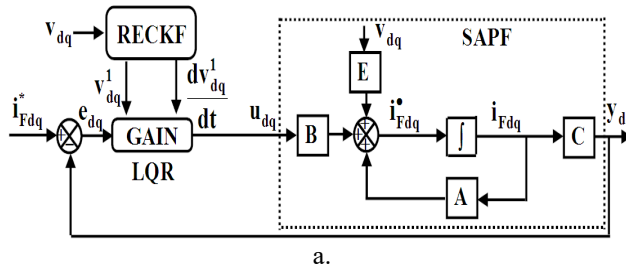


Figure 1a. Proposed RECKF-LQR based Shunt Active Power filter,  
b. Proposed Reference Current Generation



$$v_{a_k} \Rightarrow \text{KF/EKF/ECKF/RECKF} \Rightarrow [v_{a_1}, v_{a_1}^\perp]_k$$

$$v_{b_k} \Rightarrow \text{KF/EKF/ECKF/RECKF} \Rightarrow [v_{b_1}, v_{b_1}^\perp]_k$$

$$v_{c_k} \Rightarrow \text{KF/EKF/ECKF/RECKF} \Rightarrow [v_{c_1}, v_{c_1}^\perp]_k$$

b.

Figure 2a. LQR servo system structure,  
b. Identification of in phase and in quadrature components of PCC voltages

### 3. Development of SAPF

#### A. Mathematical Model

The SAPF model in the  $dq$  frame according to [4] can be expressed by equations (1) and (2), where grid voltage is considered as a disturbance. In this paper, PCC voltage dynamics are included in the model and hence the complete rotating reference frame model of SAPF [8] can be expressed by equations (3) and (4), where  $i_d, i_q$  and  $v_d, v_q$  denote the  $dq$  frame model for filter current  $i_{Fabc}$  and PCC voltages  $v_{abc}$  respectively,  $d$  is the switching function,  $\omega$  is angular frequency of the grid,  $v_{dc}$  is the dc link capacitor voltage and  $L_f, R_f$  are filter impedances.

$$\dot{i}_{dq} = Ai_{dq} + Bd_{dq} + Ev \tag{1}$$

$$y_{dq} = Ci_{dq} \tag{2}$$

where

$$A = -\begin{bmatrix} \frac{R_f}{L_f} & -\omega \\ \omega & \frac{R_f}{L_f} \end{bmatrix}, \quad B = -\begin{bmatrix} \frac{v_{dc}}{L_f} & 0 \\ 0 & \frac{v_{dc}}{L_f} \end{bmatrix}$$

$$E = \begin{bmatrix} \frac{1}{L_f} & 0 \\ 0 & \frac{1}{L_f} \end{bmatrix}, \quad C = \begin{bmatrix} 1 & 0 \\ 0 & 1 \end{bmatrix}$$

and

$$\begin{bmatrix} \dot{i}_d \\ \dot{i}_q \\ \dot{v}_d \\ \dot{v}_q \end{bmatrix} = \bar{A} \begin{bmatrix} i_d \\ i_q \\ v_d \\ v_q \end{bmatrix} + \bar{B} \begin{bmatrix} d_d \\ d_q \end{bmatrix} \tag{3}$$

$$y_{dq} = \bar{C} \begin{bmatrix} i_d \\ i_q \\ v_d \\ v_q \\ \dot{v}_d \\ \dot{v}_q \end{bmatrix} \tag{4}$$

where

$$\bar{A} = \begin{bmatrix} -\frac{R_f}{L_f} & \omega & \frac{1}{L_f} & 0 & 0 & 0 \\ \omega & -\frac{R_f}{L_f} & 0 & \frac{1}{L_f} & 0 & 0 \\ 0 & 0 & 0 & 0 & 1 & 0 \\ 0 & 0 & 0 & 0 & 0 & 1 \\ 0 & 0 & -\omega^2 & 0 & 0 & \omega \\ 0 & 0 & 0 & -\omega^2 & -\omega & 0 \end{bmatrix} \quad \bar{B} = -\begin{bmatrix} \frac{v_{dc}}{L_f} & 0 \\ 0 & \frac{v_{dc}}{L_f} \\ 0 & 0 \\ 0 & 0 \\ 0 & 0 \\ 0 & 0 \end{bmatrix} \quad \text{and} \quad \bar{C} = \begin{bmatrix} 1 & 0 & 0 & 0 & 0 & 0 \\ 0 & 1 & 0 & 0 & 0 & 0 \end{bmatrix}$$

, ,

#### 4. Robust LQR Control Strategy

The advantage of LQR over other controllers such as dead beat, hysteresis, sliding mode controller is that it is designed to minimize a performance index, which can reduce the control efforts or keep the energy of state variables under control. LQR may be considered as a robust controller, minimizing satisfactorily the state variables and the plant model must be described by

$$x_{k+1} = A_d x_k + B_d u_k \quad (5)$$

$$y_k = C_d x_k \quad (6)$$

where

$$A_d = e^{AT_s}, B_d = A^{-1}(e^{AT_s} - 1)B \text{ and } C_d = C$$

The LQR law is given by  $u_k = -Kx_k$ , which minimises the cost function

$$J = \frac{1}{2} \sum_{k=0}^{\infty} \{ x_k^T Q x_k + u_k^T R u_k \} \quad (7)$$

where  $Q$  and  $R$  are the state and control weighting matrices which are square and symmetric.

Gains  $K$  can be obtained solving the algebraic Riccati equation [23].

$$P = A_d^T P (A_d - B_d K) + Q \quad (8)$$

$$K = (B_d^T P B_d + R)^{-1} B_d^T P A_d \quad (9)$$

The LQR calculates the gain vector  $K$  by using the model specified in equation (3). According to servo system structure shown in Figure. 2(a), the state variables related to the PCC and the current references are estimated with the help of four variants of Kalman filter algorithms (KF, EKF, ECKF and proposed RECKF).

#### 5. Estimation of The PCC Fundamental and its Derivative

According to the mathematical model of SAPF specified in Section 3, the knowledge of voltages at the PCC and their derivatives are needed. It is impossible to differentiate a signal  $x$  by using the forward approximation method when the system is affected by measurement noises, spikes and other unpredictable signal disturbances. Hence, this information has to be filtered. Considering that the voltage at the PCC is predominant at the fundamental frequency, the corresponding in phase and in quadrature components can be acquired by the four auxiliary algorithms (KF, EKF, ECKF and proposed RECKF) as displayed in Figure. 2(b).

It is possible to obtain the following relations for the fundamental component of voltage at the PCC  $v_{j1k}$  and their respective derivatives  $\dot{v}_{j1k}$  that constitute state variables of the mathematical model.

$$v_{j1k} = A_{vj1k} \sin(k\omega T_s + \theta_{vj1k}) \quad (10)$$

$$\dot{v}_{j1k} = \omega \hat{v}_{j1k}^\perp = \omega A_{vj1k} \cos(k\omega T_s + \theta_{vj1k}) \quad (11)$$

where  $A_{vj1k}, \theta_{vj1k}$  are the amplitude and phase of the fundamental component of PCC voltage

at the instant  $k$ ,  $T_s$  is the sampling time,  $j$  represents the phase and  $v_{j1k}, v_{j1k}^\perp$  are the in phase and in quadrature components respectively.

*A. Signal Model and Kalman filter formulation*

A linear signal  $z_k$  of single sinusoid is represented by

$$z_k = A_{vj1k} \sin(k\omega T_s + \theta_{vj1k}) \quad (12)$$

$$\omega = 2\pi f \quad (13)$$

Hence the signal  $z_{k+1}$  can be expressed as

$$z_{k+1} = x_{1_{k+1}} = x_{1_k} \cos(k\omega T_s) + x_{2_k} \sin(k\omega T_s) \quad (14)$$

Additionally

$$x_{2_{k+1}} = -x_{1_k} \sin(k\omega T_s) + x_{2_k} \cos(k\omega T_s) \quad (15)$$

where  $x_{2_k}$  is known as the inquadature component and is orthogonal to  $x_{1_k}$ . These are represented by

$$x_{1_k} = A_{vj1_k} \sin(k\omega T_s + \theta_{vj1_k}) \quad (16a)$$

$$x_{2_k} = A_{vj1_k} \cos(k\omega T_s + \theta_{vj1_k}) \quad (16b)$$

After having obtained the state space representation of the signal specified in equation (12), KF algorithms [24] can be applied to estimate  $\hat{x}_{1_k}$  and  $\hat{x}_{2_k}$ .

### B. Signal Model and Extended Kalman filter formulation

For simplicity in formulation the signal in (12) is replaced by

$$z_k = A_{vj1_k} \cos(k\omega T_s + \theta_{vj1_k}) \quad (17)$$

It is known that the three consecutive samples of this single sinusoid will satisfy the following relationship

$$z_k - 2 \cos \omega T_s z_{k-1} + z_{k-2} = 0 \quad (18)$$

The nonlinear state space representation of the signal in equation (17) are given by

$$x_{k+1} = f(x_k) \quad (19)$$

$$y_k = g(x_k) + v_k \quad (20)$$

where  $v_k$  represents the measurement noise and

$$x_k = \begin{bmatrix} 2 \cos \omega T_s & x_{k-1} & x_{k-2} \end{bmatrix}^T$$

$$x_{k+1} = \begin{bmatrix} 1 & 0 & 0 \\ 0 & 2 \cos \omega T_s & -1 \\ 0 & 1 & 0 \end{bmatrix} x_k$$

$$f(x_k) = \begin{bmatrix} 2 \cos \omega T_s & 2 \cos \omega T_s \cdot x_{k-1} - x_{k-2} & x_{k-1} \end{bmatrix}^T$$

$$g(x_k) = 2 \cos \omega T_s \cdot x_{k-1} - x_{k-2}$$

Applying EKF theory to the nonlinear system described in equation (19) and (20), we obtain

$$\hat{x}_{k|k} = \hat{x}_{k|k-1} + K_k (y_k - g(\hat{x}_{k|k-1})) \quad (21)$$

$$\hat{x}_{k+1|k} = f(\hat{x}_{k|k}) \quad (22)$$

$$K_k = P_{k|k-1} H_k^T \cdot \left[ H_k P_{k|k-1} H_k^T + R_k \right]^{-1} \quad (23)$$

$$P_{k|k} = P_{k|k-1} - K_k H_k P_{k|k-1} \quad (24)$$

$$P_{k|k+1} = F_k P_{k|k} F_k^T \quad (25)$$

where

$$F_k = \frac{\partial f(\hat{x}_k)}{\partial \hat{x}_k} = \begin{bmatrix} 1 & 0 & 0 \\ \hat{x}_{2k} & \hat{x}_{1k} & -1 \\ 0 & 1 & 0 \end{bmatrix}, \quad H_k = \frac{\partial g(\hat{x}_k)}{\partial \hat{x}_k} = \begin{bmatrix} \hat{x}_{2k} & \hat{x}_{1k} & -1 \end{bmatrix}$$

and  $K_k$ ,  $H_k$ ,  $P_{k|k-1}$ ,  $R_k$  represent Kalman gain, observation matrix, error covariance matrix, and measurement noise covariance matrix respectively.

The inquadature component  $\hat{z}_k$  can be found from the above formulation and its correspondent in phase component can be obtained by a 90 degree phase shifter block.

### C. Signal Model and Extended Complex Kalman Filter Formulation

The signal formulation in equation (12) can be represented as a complex type, i.e.,

$$z_k = (-0.5i) \left( A_{vj1k} e^{i(k\omega T_s + \theta_{vj1k})} \right) + (0.5i) \left( A_{vj1k} e^{-i(k\omega T_s + \theta_{vj1k})} \right) \quad (26)$$

The complex type state variable  $x_k$  can be given as

$$x_{1k} = e^{i\omega T_s} \quad (27a)$$

$$x_{2k} = A_{vj1k} e^{i(k\omega T_s + \theta_{vj1k})} \quad (27b)$$

$$x_{3k} = A_{vj1k} e^{-i(k\omega T_s + \theta_{vj1k})} \quad (27c)$$

The nonlinear state space equations can be represented as

$$x_k = f(x_{k-1}) \quad (28)$$

$$y_k = g(x_k) + v_k \quad (29)$$

where

$$f(x_{k-1}) = \begin{bmatrix} x_{1(k-1)} & x_{1(k-1)} & x_{2(k-1)} & \frac{x_{3(k-1)}}{x_{1(k-1)}} \end{bmatrix}^T \quad (30)$$

The recursion process of the ECKF for estimating the signal parameters of sinusoid waves is given below.

$$\tilde{x}_k = f(\hat{x}_{k-1}) \quad (31)$$

$$M_k = F_k P_{k-1} F_k^T + Q_k \quad (32)$$

$$\hat{x}_k = \tilde{x}_k + K_k (y_k - H_k \tilde{x}_k) \quad (33)$$

$$K_k = M_k H_k^T \left[ H_k M_k H_k^T + R_k \right]^{-1} \quad (34)$$

$$P_k = M_k (I - K_k H_k) \quad (35)$$

where the symbols  $\sim$  and  $\hat{\phantom{x}}$  stand for the predicted and estimated values respectively,  $M_k$  and  $P_k$  represent the predicted and estimated error covariance respectively.  $F_k$  and  $H_k$  are described as

$$F_k = \frac{\partial f(\hat{x}_{k-1})}{\partial \hat{x}_{k-1}} = \begin{bmatrix} 1 & 0 & 0 \\ \hat{x}_{2(k-1)} & \hat{x}_{1(k-1)} & 0 \\ -\hat{x}_{3(k-1)} / \hat{x}_{1(k-1)}^2 & 0 & 1 / \hat{x}_{1(k-1)} \end{bmatrix} \quad (36)$$

$$H_k = \frac{\partial (g(x_k))}{\partial x_k} = [0 \quad -0.5i \quad 0.5i] \quad (37)$$

The parameters of frequency  $\hat{f}_k$ , amplitude  $\hat{A}_{vj1k}$  and phase angle  $\hat{\theta}_{vj1k}$  can be given by

$$\hat{f}_k = \frac{1}{2\pi T_s} \left[ \text{Im} (\ln(\hat{x}_{1k})) \right] \quad (38)$$

$$\hat{A}_{vj1k} = |\hat{x}_{2k}| \quad (39)$$

$$\hat{\theta}_{vj1k} = \text{Im} \left[ \ln \left( \frac{\hat{x}_{2k}}{|\hat{x}_{2k}| \times (\hat{x}_{1k})^k} \right) \right] \quad (40)$$

Using above parameters  $\hat{f}_k$ ,  $\hat{A}_{vj1k}$ ,  $\hat{\theta}_{vj1k}$  the in phase fundamental component can be identified and the corresponding in quadrature component can be obtained with a 90 degree phase shifter block.

#### D. Signal Model and Proposed Robust Extended Complex Kalman Filter Formulation

The signal model and filter formulations in RECKF are same as in ECKF. The only difference is in the measurement error covariance matrix  $R_k$ , which is the inverse of the weighting  $W_k$ , i.e.

$$R_k = W_k^{-1} \quad (41)$$

$$W_k = W_{k-1} e^{-(y_k - H_k \tilde{x}_k)^2} \quad (42)$$

where the exponential term  $e^{-(y_k - H_k \tilde{x}_k)^2}$  is the proposed robust exponential function and the variable  $R_k$  is replaced in equation (34). When any grid disturbances occur at the PCC, the residual vector  $(y_k - H_k \tilde{x}_k)$  increases faster due to the inclusion of a 'square term' in the proposed exponential function. Consequently, the value of proposed robust exponential function decreases faster and finally a fast reduction of weighting and mitigation of error can be achieved.

### 6. Proposed Reference Current Generation

The proposed reference current generation scheme is represented in Figure. 1(b). The reference source currents that are used to decide the switching of the SAPF have two parts: one is the real fundamental-frequency component of the load current, which is estimated using the proposed RECKF and another component, which corresponds to the losses in the SAPF, is also estimated using our proposed RECKF over the dc voltage of SAPF.

Firstly, a difference between the estimated fundamental amplitude of source current and load current is realized and then adding this value with the fundamental amplitude of load current contributes to desired peak value of source current  $i_{sm}$ . Finally, reference source current  $i_{Sabc}^*$  is created via modulation of  $i_{sm}$  with the estimated in phase fundamental component of PCC voltage in p.u. value ( $U_{abc}$ ) as depicted in equation (43). For the sake of LQR implementation, the reference compensating currents  $i_{Fabc}^*$  can be traced through equation (44).

$$i_{Sabc}^* = i_{sm} \times U_{abc} \quad (43)$$

$$i_{Fabc}^* = i_{Labc} - i_{Sabc}^* \quad (44)$$

The estimation approach is same as described in Section 5 for PCC voltages.

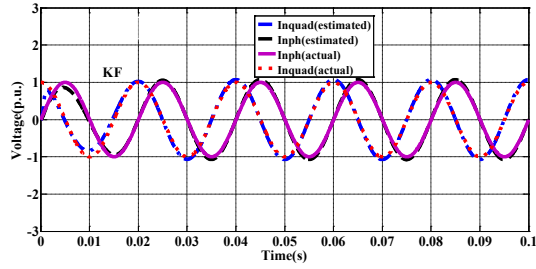
## 7. Results and Discussions

### A. Simulation Results

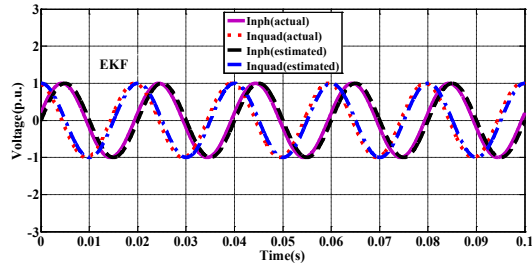
In order to evaluate the efficacies of the proposed method, the system presented in Figure. 1 is implemented using MATLAB/simulink. In the simulation studies a three phase voltage supply has been applied upon a typical nonlinear load composed of a three-phase diode rectifier bridge feeding RL load. The system parameters are summarized in Table 1, where  $f_{sw}$  is the switching frequency,  $L_s$  and  $R_s$  correspond to the source impedance,  $L_f$  and  $R_f$  correspond to the filter impedance,  $V_s$  is the system voltage,  $v_{dc}^*$  is the reference dc bus voltage, and  $f$  is the system frequency.

Table 1. Simulation Parameters

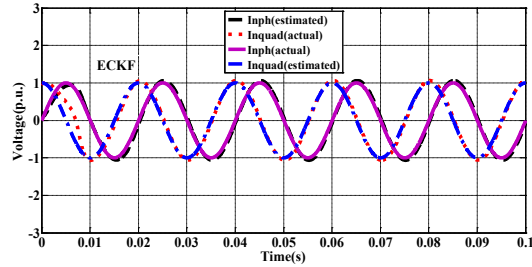
$f_{sw}$	12 kHz	$f$	50 Hz
$L_s$	1 mH	$R_s$	0.1 $\Omega$
$L_f$	2.7 mH	$R_f$	0.1 $\Omega$
$V_s$	100V	$v_{dc}^*$	220V



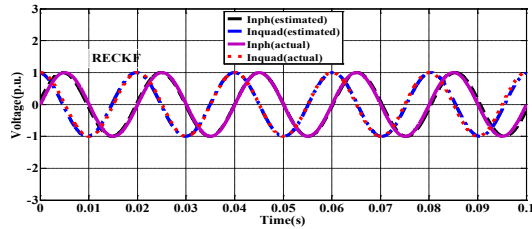
a. KF



b. EKF

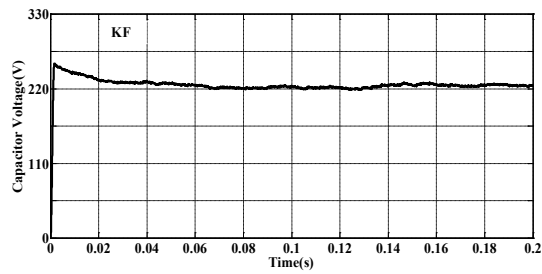


c. ECKF

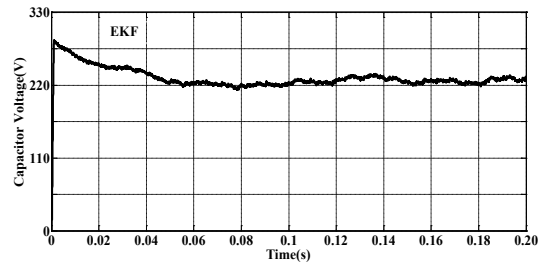


d. Proposed RECKF

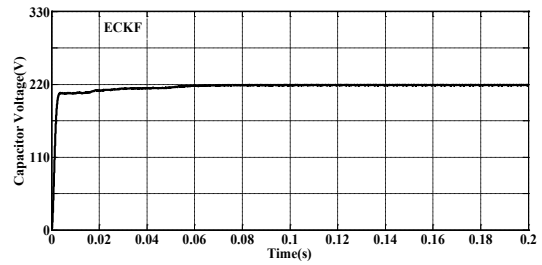
Figure 3. Waveform of in phase and in quadrature component at PCC



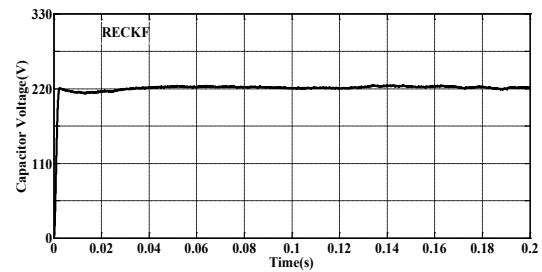
a. KF



b. EKF



c. ECKF



d. Proposed RECKF

Figure 4. Waveform of dc link capacitor voltage

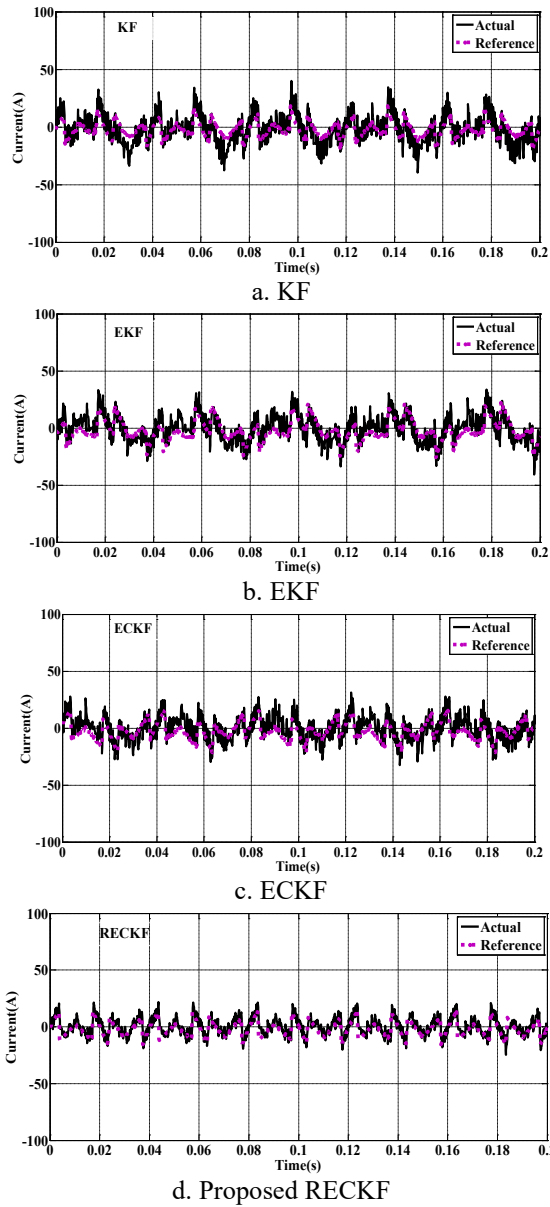


Figure 5. Waveform of reference and actual compensating current

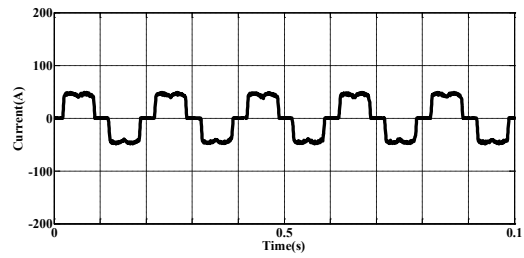


Figure 6. Waveform of Load Current

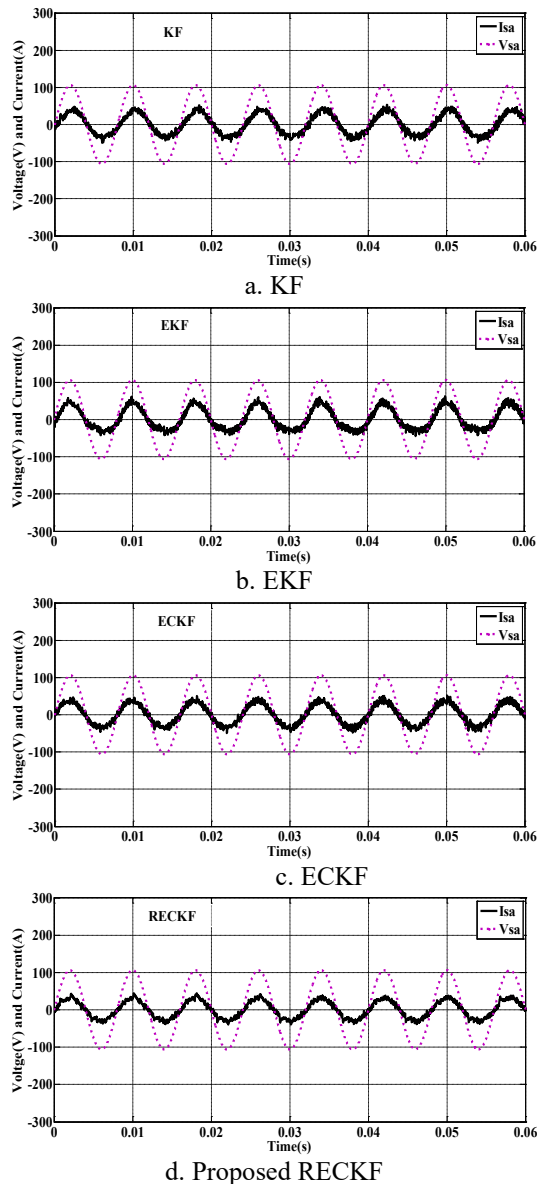


Figure 7. Waveform of source voltage and source current after compensation

In the simulation, zero mean white noise was considered for process noise and the filtered error covariance matrix  $P_0$  was selected to be diagonal with the value of  $10 pu^2$ . The measurement error covariance matrix  $R_0$  was selected to be  $1.0 pu^2$  to represent an inaccurate measurement and the process error covariance matrix  $Q_0$  was fixed to be  $0.0001 pu^2$ . The selection of Q and R matrix in LQR design is based upon performance specifications, and a certain amount of trial and error is required with an interactive computer simulation before arriving at satisfactory design results. Since the matrix Q and R are symmetric, six distinct elements in Q and two distinct elements in R need to be selected. The matrices Q and R should be positive definite. The value of the elements in Q and R are associated with their contribution towards cost function J.

$$Q = \begin{bmatrix} 3700 & 0 & 0 & 0 & 0 & 0 \\ 0 & 4970 & 0 & 0 & 0 & 0 \\ 0 & 0 & 0 & 0 & 0 & 0 \\ 0 & 0 & 0 & 0 & 0 & 0 \\ 0 & 0 & 0 & 0 & 0 & 0 \\ 0 & 0 & 0 & 0 & 0 & 0 \end{bmatrix} \quad R = \begin{bmatrix} 1 & 0 \\ 0 & 1 \end{bmatrix} \quad (45)$$

The simulation results employing four Kalman algorithms (KF, EKF, ECKF, and proposed RECKF) are presented. Figure. 3 depicts the in phase and in quadrature components of the PCC voltage estimated using above four algorithms. As perceived through Figure. 3(a) and Figure. 3(c), it takes about 0.015 sec and 0.01sec for the actual and estimated values to exactly tally in case of KF and ECKF respectively. In EKF approach as revealed in Figure. 3(b), there is a small phase difference between the actual and estimated values. But the real and estimated values of in phase and in quadrature components tie in with the proposed RECKF as detected through Figure. 3(d).

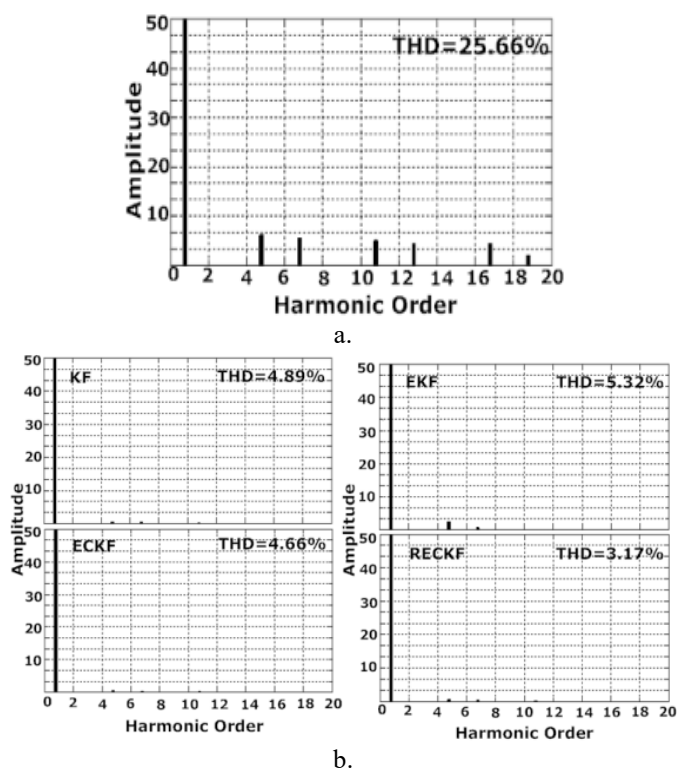


Figure.8 THD Spectrum of the source current a) before compensation and b) after compensation with KF, EKF, ECKF, Proposed RECKF

The dc voltage profiles for different variants of KF algorithms are presented in Figure. 4 (a), (b), (c) and (d). As seen from Figure. 4, there are small ripples in the capacitor voltage in case of KF and EKF, but no ripples are found in case of ECKF and proposed RECKF. Moreover they are evaluated in terms of dc voltage settling time, which are specified in Table 2 and it can be seen that the settling time is very less ( $\approx 0.03$ sec) in case of proposed RECKF exhibiting better regulation of capacitor voltage. The actual current output of the SAPF for phase 'a' is superimposed with its respective reference and revealed in Figure. 5 (a), (b), (c) and (d) for four auxiliary algorithms. From outcomes, it is inferred that the filter injected current harmonics track their references with high levels of accuracy and this accuracy is measured in terms of 'tracking

error’ as summarized in Table 3. From Figure. 5 and Table 3, it is clear that the error is found to be maximum ( $\approx 46.4\%$ ) at EKF whereas minimum ( $\approx 9.5\%$ ) at proposed RECKF.

The load current waveform is depicted in Figure. 6. Figure. 7 (a), (b), (c) and (d) compare the current quality obtained with different variants of Kalman filter algorithms after compensation with SAPF. As can be seen, the source currents are sinusoidal and balanced with power factor close to the unity. But these are compared on the basis of their respective spectrum analysis using Fast Fourier Transform (FFT).The spectrum analysis of load and source currents for above four Kalman filter algorithms are depicted in Figure. 8 (a), (b), (c) and (d). It is analysed that the total harmonics distortion (THD) of the source current is reduced from 25.17% to 4.89%, 5.32%, 4.66% and 3.17% after compensation with KF, EKF, ECKF and proposed RECKF respectively. These results confirm the superiority of proposed RECKF in terms of harmonics compensation of SAPF.

Table 2 (Measurement of  $v_{dc}$  settling time)

Algorithms	$v_{dc}$ settling time in sec
KF	0.07
EKF	0.08
ECKF	0.06
Proposed RECKF	0.03

Table 3 (Measurement of Tracking Error)

Algorithms	Tracking Error
	$= \frac{I_{Faref} - I_{Fa}}{I_{Fa}} \times 100\%$
KF	37.5
EKF	46.4
ECKF	43.2
Proposed RECKF	9.5

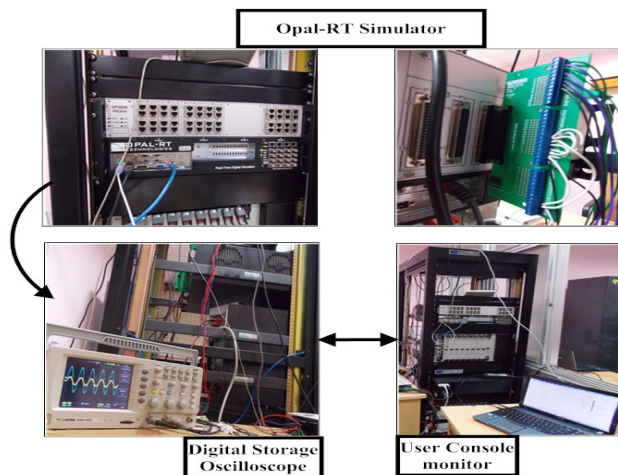
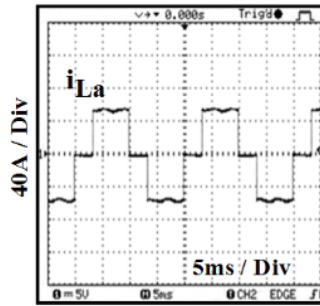
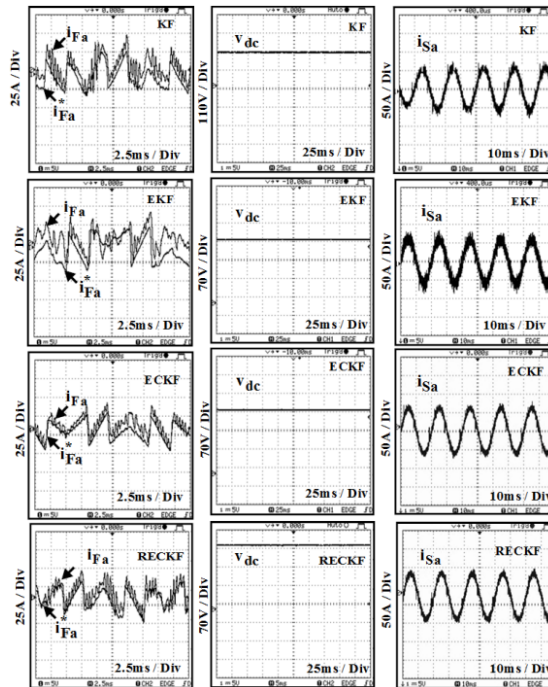


Figure 9. RT-LAB real-time Simulator

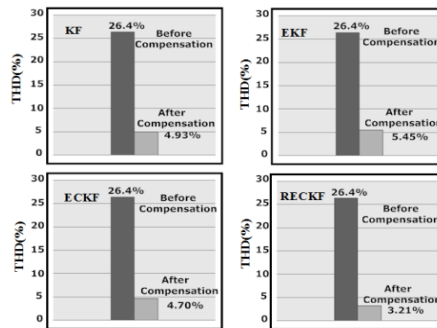
B. Real-Time Opal-RT Results



a.



b.



c.

Figure 10. RT-LAB results, a) Load Current, b) Reference current tracking, Capacitor voltage and Source current waveforms for KF, EKF, ECKF and proposed RECKF respectively, c) Compensation effects of KF, EKF, ECKF and proposed RECKF respectively

Table 4 (Calculation of THD%)

SAPF system	THD% of the source current after compensation ( THD% of the source current before Compensation (26.4%))
KF-LQR	4.93
EKF-LQR	5.45
ECKF-LQR	4.70
Proposed RECKF-LQR	3.21

The real-time results obtained from the implementation of the proposed SAPF algorithm on Opal-RT are presented in this section. Figure. 9 shows the real-time simulation machine along with a console monitor and digital storage oscilloscope interface. The Opal-RT Platform [25, 26] enables the parallel simulation of power drives and electric circuits on clusters of PC running quick UNIX (QNX) or RT-Linux operating systems. Using standard SIMULINK models, RT-LAB builds computation and communication tasks necessary to make parallel simulation of electrical systems with standard PCs and communication links. The Opal-RT allows developers to prove their ideas, prototypes and final products in a realistic environment. It is an ideal tool for the design, development and testing of power system protection and control schemes. Figure. 10 (a) displays the real-time Opal-RT result for load current. Further, the real-time results for reference and actual compensating current, capacitor voltage and source current are represented in Figure. 10 (b) and compensation effect of the KF-LQR, EKF-LQR, ECKF-LQR and proposed RECKF-LQR based SAPF system are demonstrated in Figure. 10 (c). The THD results for above KF algorithms are expressed in Table 4. From the tabulation it is analyzed that THD of the source currents are lowered from 26.4% to 4.93%, 5.45%, 4.70% and 3.21% after compensation with LQR based SAPF system in case of KF, EKF, ECKF and proposed RECKF approach respectively signifying an outstanding performance of proposed RECKF-LQR towards the expansion of SAPF. These Opal-RT results are quite agreed with the simulation results attained.

## 8. Conclusions

In this paper, a new SAPF has been proposed that employs proposed RECKF algorithm for providing estimation of states together with the design of an optimal LQR that regulates the dc bus voltage without any external PI controller loop. The proposed algorithm generates appropriate references for the LQR under grid disturbances such as voltage distortion, frequency deviation and measurement noise. In order to verify the accuracy and robustness of the proposed RECKF-LQR based SAPF, a comparative evaluation has been made using four variants of Kalman filtering algorithms (KF, EKF, ECKF and RECKF). The overall performances of four different approaches such as KF-LQR, EKF-LQR, ECKF-LQR and proposed RECKF-LQR based SAPF systems are analysed through simulation as well as real-time Opal-RT platforms. The results obtained demonstrate that the proposed RECKF-LQR approach provides excellent performance in terms of dc voltage tracking, reference current tracking as well as current harmonics mitigation in the SAPF system.

## 9. References

- [1]. H. Akagi, "New trends in active filters for power conditioning," *IEEE Trans. Ind. Appl.*, vol. 32, no. 32, pp. 1312–1332, Nov./Dec. 1996.
- [2]. R. K. Patjoshi and K. K. Mahapatra, "Resistive Optimization and Nonlinear Variable gain Fuzzy based Hysteresis Control Strategy for Unified power quality conditioner", *International Journal of Electrical power and Energy system*, vol.83, no.12, PP.352-363, 2016.

- [3]. R. K. Patjoshi and K. K. Mahapatra, "High- performance unified power quality conditioner using non-linear sliding mode and new switching dynamics control strategy." *IET Power Electron.* vol. 10, no. 8, pp. 863-874, Jun 2017.
- [4]. B. Kedjar and K. Al-Haddad, "DSP-based implementation of an LQR with integral action for a three-phase three-wire shunt active power filter," *IEEE Trans. Ind. Electron.*, vol. 56, Aug. 2009.
- [5]. F. Huerta, D. Pizarro, and A. Rodriguez, "LQG servo controller for the current control of grid connected voltage-source converters," *IEEE Trans. on Ind. Electron.*, vol. 59, no. 11, pp. 4272–4284, Aug. 2012.
- [6]. R. K. Patjoshi and K. K. Mahapatra, "High-performance unified power quality conditioner using command generator tracker-based direct adaptive control strategy," *IET Power Electronics*, vol. 9, no. 6, pp. 1267-1278, May 2016.
- [7]. K. H. Kwan, P. L. So, and Y. C. Chu, "An output regulation-based unified power quality conditioner with Kalman filters," *IEEE Trans. Ind. Electron.*, vol. 59, no. 11, pp. 4248–4262, 2012.
- [8]. J. M. Kanieski, R. Cardoso, and H. A. Grundling, "Kalman filter based control system for power quality conditioning devices", *IEEE Trans. Ind. Electron.*, vol. 60, no.11, pp. 5214-5227, Nov. 2013.
- [9]. R. Panigrahi and B. Subudhi. "Performance Enhancement of Shunt Active Power Filter Using a Kalman Filter-Based H-infinity Control Strategy." *IEEE Transactions on Power Electron.*, vol. 32, no. 4, pp. 2622-2630, Apr. 2017.
- [10]. P. K. Dash, G. Panda, and A. Routray, "An extended complex Kalman filter for frequency measurement of distorted signals", *IEEE Trans. Instrum. Meas.*, vol. 49, no. 4, pp.746-753, Aug. 2012.
- [11]. K. Nishiyama, "A nonlinear filter for estimating a sinusoidal signal and its parameters in white noise: on the case of a single sinusoid", *IEEE Trans. Signal Processing*, vol.45, no.4, pp.970-981, Apr. 1997.
- [12]. V. V. Terzija, N. B. Djuric, and B. D. Kovacevic, "Voltage phasor and local system frequency estimation using Newton type algorithm," *IEEE Trans. Power Del.*, vol. 9, no. 3, pp. 1368–1374, Jul. 1994.
- [13]. R. Panigrahi, P. C. Panda and B.Subudhi, "A robust extended complex kalman filter and sliding-mode control based shunt active power filter." *Electric Power Components and Systems*, vol. 42, no. 5, pp. 520-532, Feb. 2014.
- [14]. A. Routray, A. K. Pradhan, and K. P. Rao, "A novel Kalman filter for frequency estimation of distorted signal in power systems," *IEEE Trans. Instrum. Meas.*, vol. 51, no. 3, pp. 469–479, Jun. 2002.
- [15]. R. K. Patjoshi and K. K. Mahapatra, "Performance analysis of shunt active power filter using PLL based control algorithms under distorted supply condition," *Proc. IEEE Students Conference on Engineering and Systems (SCES)*, Allahabad, 2013, pp. 1-6.
- [16]. G. G. Rigatos, "A derivative free kalman filtering approach to state estimation based control of nonlinear systems," *IEEE Trans. Indust. Electron.*, vol. 59, no. 10, pp. 3987–3997, Oct. 2012.
- [17]. R. K. Patjoshi, R. Panigrahi, "Shunt Active Power Filter Employing Robust Extended Complex Kalman Filter based Linear Quadratic Regulator Control Strategy for Power Quality Enhancement," *Journal of Power Technology*, vol.100, no.2, pp.231-237, 2020.
- [18]. R. Panigrahi, P. C. Panda and B.Subudhi, "New strategy for generation of reference current in active power filters with distortion in line voltage," *Proceedings of 7th IEEE International Conference on Industrial and Information Systems (ICIIS)*, Chennai, 2012.
- [19]. R. K. Patjoshi and K. K. Mahapatra, "Power Quality Enhancement Using Fuzzy Sliding Mode based Pulse Width Modulation Control Strategy for Unified Power Quality Conditioner", *International Journal of Electrical power and Energy system*, vol.84, no.1, PP.153-167, 2017.

- [20]. C. H. Huang, C. H. Lee, and Y. J. Wang, "A robust technique for frequency estimation of distorted signals in power systems," *IEEE Trans. Instrum. Meas.*, vol. 59, no. 8, pp. 2026-2036, Aug. 2010.
- [21]. R. Panigrahi, S. Rauta, and P. C. Panda, "A Robust extended complex Kalman filter applied to distorted power system signals for frequency estimation," in *Proc. IEEE Int. Conf. Power Sys.*, pp. 126-131, 2009.
- [22]. R. Panigrahi and B.Subudhi, "A Robust LQG servo control strategy of shunt active power filter for power quality enhancement," *IEEE Trans. on Power Electron.*, vol. 31, no. 4, pp.2860-2869, 2016.
- [23]. C. L. Phillips and H. R. Nagle, *Digital Control System Analysis and Design*. Prentice-Hall, 1995.
- [24]. R. Cardoso, H. Pinheiro, and H. A. Grundling, "Kalman filter based synchronization methods", *IET Gener. Transm. Distrib.*, vol. 2, no. 4, pp.542-555, 2008.
- [25]. R. Panigrahi, B.Subudhi, and P. C. Panda, "Model predictive based shunt active power filter with a new reference current estimation strategy," *IET Power Electron.*, vol. 8, no. 2, pp.221-233, 2015.
- [26]. RT-Lab Professional. Available at <http://www.opal-rt.com/product/rtlab-Professional>



**Rakhee Panigrahi** received the B.E. degree in Electrical Engineering from the Veer Surendra Sai University of Technology Burla, Odisha, India and the M.Tech and Ph.D. degrees in Electrical Engineering from the National Institute of Technology, Rourkela, India, in 2009 and 2015, respectively. She is currently an Asst. Professor in the Department of Electrical Engineering, Biju Patnaik University of Technology, Parala Maharaja Engineering College, Berhampur. Her research interests include advanced control approach, estimation techniques with application to power quality, renewable energy and

grid integrated microgrid system.



**Rajesh Kumar Patjoshi** received the B.E. degree in Electronics and Telecommunication Engineering from the Amaravati University, India and the M.Tech and Ph.D. degrees in Electronics and Communication engineering from the National Institute of Technology, Rourkela, India, in 2010 and 2015, respectively. He is currently an Associate Professor in the Department of Electronics and communication Engineering, National Institute of Science and Technology, Berhampur. His research interests include power quality enhancement towards grid integrated renewable energy source and microgrid

system, network control system, embedded systems, VLSI design for artificial intelligence, Low power and RF VLSI design.